

MALAYSIAN JOURNAL OF ANALYTICAL SCIENCES

Published by The Malaysian Analytical Sciences Society

ISSN 1394 - 2506

MOLECULAR AND ELECTRONIC STRUCTURES OF A NEW RUTHENIUM-TUNGSTEN BIMETALLIC COMPLEX USING DENSITY FUNCTIONAL THEORY CALCULATIONS

(Struktur Molekul Dan Elektronik Kompleks Dwilogam Rutenium-Tungsten Berdasarkan Pengiraan Teori Fungsi Ketumpatan)

Khuzaimah Arifin¹*, Hasmida Bt. Abdul Kadir^{1,3}, Lorna Jeffery Mingg Van Ramli Wan Daud^{1,2}, Mohammad B. Kassim^{1,3}

¹Fuel Cell Institute

²Department of Chemical and Process Engineering

³School of Chemical Sciences and Food Technology, Faculty of Science and Technology

Universiti Kebangsaan Malaysia, 43600 UKM Bangi, Selangor, Malaysia

*Corresponding author: khuzaim@ukm.edu.my

Received: 5 February 2016; Accepted: 22 April 2016

Abstract

A potential dye sensitizer material for solar cell composed of a ruthenium-(4, 4'dimethyl-2, 2'-bipyridine)-isothiocyanato-tungsten-[bis-(phenyl-1, 2-ethilenodithiolenic)] bimetallic complex structure was successfully developed using Density Functional Theory (DFT) calculations. The optimal structure was realized by calculations using the generalized gradient approximation (GGA) framework in a double numeric plus polarization (DNP) basis set using the following three functional methods: Becke-Pardew (BP), Becke-Lee-Yang-Parr (BLYP) and Perdew-Burke-Ernzerhof (PBE). The PBE calculation gave a structure with bond lengths and angles that approximated the experimental data. The restricted-spin calculation of PBE found that BM has 339 molecular orbitals in which the highest occupied molecular orbital (HOMO) and lowest unoccupied molecular orbital (LUMO) are located at orbital numbers 312 and 313, respectively. The HOMO was delocalized over the $W(S_2C_2)$ ring, the ruthenium metal center and the thiocyanate bridging ligand. In contrast, the LUMO was found mainly at the bipyridyl ligand with a small contribution from the ruthenium metal center. Electron excitation from the HOMO \rightarrow LUMO occurred at 2964 nm with an excitation energy of 0.42 eV, which is depicted by the charge transfer from one metal to another (intervalence charge transfer, IVCT) or as a manifestation of the NCS bridging ligand.

Keywords: density functional theory, bimetallic, thiocyanate, bridging ligand

Abstrak

Pembangunan struktur molekul kompleks dwilogam rutenium-(4,4)'dimetil-2,2'-bipiridina)-isotiosianat-tungsten[bis-(fenil-1,2-etilenoditiolena)] (BM) telah dilakukan menggunakan kaedah pengkomputeran Teori Fungsi Ketumpatan (DFT) berdasarkan data yang diperoleh dari eksperimen. Untuk mendapatkan struktur yang optimum, pengiraan telah dilakukan dengan menggunakan pendekatan gradien menyeluruh (GGA) dengan set asas pengutuban tambahan gandaan angka (DNP) pada tiga kaedah fungsian; Becke-Pardew (BP), Becke-Lee-Yang-Parr (BLYP) dan Perdew-Burke-Ernzerhof (PBE). Pengiraan menggunakan fungsian PBE menghasilkan struktur dengan panjang dan sudut ikatan yang paling mendekati nilai eksperimen. Hasil pengiraan spin terhad dengan PBE mendapati bahawa kompleks BM memiliki 339 orbital molekul, di mana orbital molekul berisi tertinggi (HOMO) dan orbital molekul tak berisi terendah (LUMO) masing-masing berada pada orbital molekul 312 dan 313. Orbital HOMO kompleks dwilogam BM didapati dinyah setempat pada gelang W(S_2C_2), logam pusat Ru serta ligan penghubung NCS. Sebaliknya, orbital LUMO sebahagian besarnya berada pada ligan bipiridil dengan sedikit sumbangan dari logam pusat Ru. Tenaga pengujaan elektron dari HOMO \rightarrow LUMO wujud sebagai puncak penyerapan pada 2964 nm

Khuzaimah et al: MOLECULAR AND ELECTRONIC STRUCTURES OF A NEW RUTHENIUM-TUNGSTEN BIMETALLIC COMPLEX USING DENSITY FUNCTIONAL THEORY CALCULATIONS

dengan tenaga pengujaan 0.42 eV yang berpadanan dengan peralihan cas daripada logam kepada logam (peralihan cas antara velensi, IVCT) yang menyokong peranan NCS sebagai ligan titian.

Kata kunci: teori fungsi ketumpatan, kompleks dwilogam, thiosianat, ligan penghubung

Introduction

Computational chemistry investigations have been used in many fields, such as in solar cell material development [1], batteries [2], sensors [3] and thermoelectric materials [4]. The investigation can be used to identify the structure and properties of the crystal and bulk molecule as well as the thin film surface; it can also be used to model the chemical reactions on the structure surface for a more detailed understanding [5, 6]. The computational chemistry methods and the ability of each method to analyze the structure and predict the properties of molecules have been widely discussed, including the density functional theory (DFT) method. The DFT method has been used to successfully and accurately study various properties of molecules in the ground state, including transition metal complex molecules.

The ruthenium-(4,4'dimethyl-2,2'-bipyridine)-isothiocyanato-tungsten-[bis-(phenyl-1,2-ethilenodithiolenic)] bimetallic complex, abbreviated BM, was successfully synthesized, and its properties were investigated as a potential dye sensitizer molecule for TiO₂ [7, 8]. Because the acquisition of a suitable BM single crystal for X-ray diffraction studies has been unsuccessful, in this study, the theoretical development of the BM molecular structure was investigated. DFT analysis used for in-depth studies was performed on the optimized molecular structure. The development of the molecular structure using a theoretical calculation is similar in principal to the X-ray diffraction refinement of a single crystal molecule, which defines the most stable structure at the lowest energy or stationary state. The molecular orbital configuration and the optical properties of the lowest energy BM structure were reported for various parameter calculations.

Materials and Methods

Computational details

The molecular structure and density functional theory (DFT) calculations were performed using Microsoft visualizer and the DMol³ module in Bolivia Materials Studio 7.0 software. All of the calculations were performed using the self-consistent field (SCF) method on a spin polarization system with the multiplicity set to auto for all of the core electron treatments. The SCF is a repetition of Hatree Fock calculations on all of the electrons until the effective electrostatic field does not further change or converges. For the DFT calculation, an approximation should be performed because an energy function is not precisely known. In this study, the generalized gradient approximation (GGA) was used with varying correlation functional methods, such as Pardew Backe (BP), Beckie (B), gradient-corrected correlation of Lee-Yang-Parr (LYP) and the exchange correlation Perdew-Burke-Ernzerhof (PBE) [9,10,11]. Double numerical plus polarization (DNP), which is comparable to 6-31G ** of the Gaussian basis set was used [12]. The entire geometry optimization process in this study was performed with fine quality. The geometry optimization was reiterated until the structure reached its lowest energy state.

Vibrational frequency analysis was used to confirm the energy state of the structure in every geometry optimization process. The absence of imaginary frequencies in the optimization results indicates that the structures are already in a stationary state [13]. In addition, the comparison results of vibration frequency analysis calculations with experimental FTIR analysis results were used as supplementary information for the confirmation of the molecular structure. The result was quality examined by comparing the bond lengths and angles of the calculation results with a similar molecular structure that has been reported. Analysis of the molecular orbital calculations and the optical properties was performed on the optimized structures of the molecule using the time dependence of the density functional theory (TD-DFT) method [14].

Results and Discussion

Molecular structure

The molecular structure of BM was constructed from two octahedral precursors. The molecular structures of the precursors were derived from X-ray single crystal data of similar molecules with ligand modification (Figure 1). Both of the precursor structures were optimized to the stationary state and placed adjacent to each other with the

thiocyanate ligands of ruthenium-[bis(4,4'-dimethyl-2,2'-bipyridyl)-isothiocyanato], abbreviated as M1 complex, and the carbonyl ligands of the tungsten dithiolene carbonyl complex $[W(S_2C_2Ph_2)_2(CO)_2]$ (M2) facing each other. The carbonyl ligands of complex M2 were then removed, and each S atom on the -NCS- ligands of complex M1 was connected to the tungsten atom of complex M2, forming double -NCS- bridging ligands. The bond lengths of W-S and S-Ru were arranged to approach normal lengths. The BM structure was then optimized several times until no imaginary frequencies were found using various parameters.

Figure 1. The reaction scheme for preparation of BM

To ensure that the complex structure agreed with the experimental data, the frequency vibration spectra were compared with FTIR experimental data (Figure 2). Although the peaks of the harmonic vibration frequency spectra calculation and those from the FTIR experiment were not exactly in the same position, the important peaks, such as N–H, C–C aromatic, and –NCS, among others, were present in both of the spectra. Most of the peaks of the spectrum calculation appeared at a lower energy of approximately 200 cm⁻¹ compared with the FTIR experimental peak frequencies. This result is because the environmental factors of the experiment cannot be perfectly modeled, such as the presence of residual solvent molecules that might affect the experimental spectrum. In this study, the optimization calculation was processed under vacuum conditions. The optimized structure of BM is similar to the bimetallic complex with the double thiocyanate ligand structure reported by Eran et al. [15]. Eran has reported a homobimetallic complex of Pt connected to double thiocyanate ligands in which each Pt was connected to –S and N– of the thiocyanate.

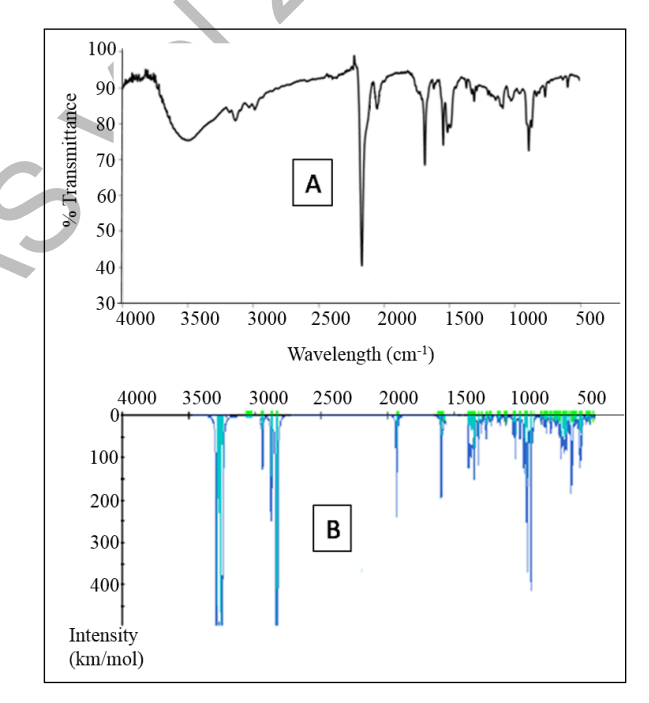


Figure 2. Comparison of FTIR experiment (A) and harmonic vibrational frequencies spectrum (B) of BM

The BM was optimized using three different GGA functionals, which produced a slightly different geometrical structure (Figure 3). The total energy consumption during the optimization process and the band gap energy produced are listed in Table 1. All of the optimized structures have two metals in the center of the perpendicular plane. All of the bipyridine and dithiolene ligands chelated each metal center, which distorted the octahedral structure. The optimized structure of BM using BLYP and PBE resulted in a similar structure in which the geometry of the W metal center was more closely distorted to trigonal prismatic. The W-S bond length of the BLYP calculation result was generally longer than that of the BP and PBE results. All of the bond length and angle calculation results are summarized in Table 2.

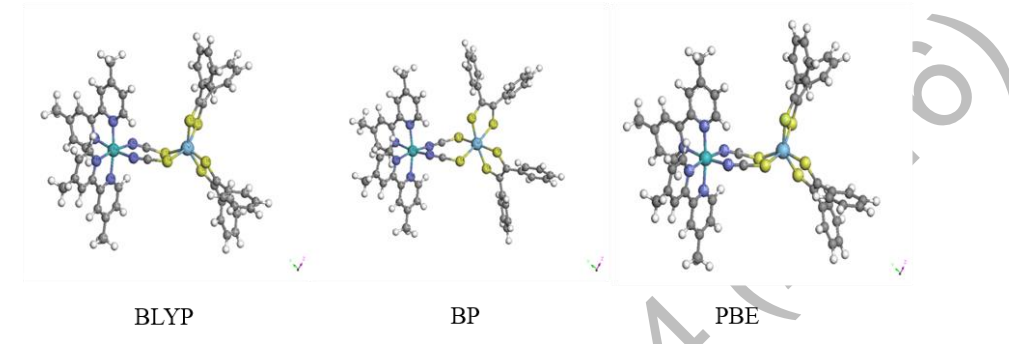


Figure 3. The optimize molecular structure of BM using three different GGA functionals calculation

Table 1. Energy calculation for structural optimization of two isomers of BM at three different DFT functional calculations

GGA Functional	Energy Optimization (Ha)	E-HOMO (eV)	E-LUMO (eV)	Band gap energy (eV)
BLYP	-24538.44	-3.527	-3.125	0.402
BP	-24540.34	-4.575	-3.236	1.339
PBE	-24534.05	-3.671	-3.288	0.383

Table 2. Comparison of selected bond lengths (Å) and angles (°) of optimized BM geometries using three DFT functional calculations

Rond Longth (Å)	GGA		Dand Langth (Å)	GGA			
Bond Length (Å)	BLYP	BP	PBE	Bond Length (Å)	BLYP	BP	PBE
W-S(1)	2.388	2.427	2.406	S(5)-C(37)	1.766	1.764	1.749
W-S(2)	2.432	2.417	2.413	S(6)-C(46)	1.765	1.766	1.756
W-S(5)	2.406	2.416	2.414	Ru-N(1)	2.114	2,085	2.076
W-S(6)	2.405	2.413	2.399	Ru-N(2)	2.126	2.098	2.099
W-S(3)	2.699	2.599	2.617	Ru-N(3)	2.128	2.113	2.099
W-S(4)	2.675	2.647	2.601	Ru-N(4)	2.125	2.097	2.091
S(3)-C(2)	1.703	1.666	1.657	Ru-N(5)	2.127	2.097	2.090
S(4)-C(1)	1.752	1.665	1.661	Ru-N(6)	2.138	2.113	2.109
S(1)-C(9)	1.766	1.760	1.752	N(1)-C(1)	1.181	1.181	1.182
S(2)-C(10)	1.761	1.760	1.748	N(2)-C(2)	1.184	1.183	1.186

Table 2 (cont'd). Comparison of selected bond lengths (Å) and angles (°) of optimized BM geometries using three DFT functional calculations

Bond Angle (°)				Bond Angle (°)			
S(1)-W-S(2)	79.25	79.76	79.48	C(1)-N(1)-Ru	153.61	151.67	152.00
S(5)-W-S(6)	79.92	80.16	80.15	C(2)-N(2)-Ru	151.25	149.19	143.73
S(3)-W-S(4)	92.44	95.61	94.31	N(1)-Ru- $N(2)$	81.19	79.62	80.66
S(1)-W-S(5)	120.17	113.8	117.5	N(3)-Ru- $N(4)$	77.39	77.87	78.12
S(1)-W-S(6)	85.78	84.63	85.93	N(5)-Ru- $N(6)$	77.30	77.89	78.04
S(1)-W-S(3)	82.65	83.22	84.08	N(1)-Ru-N(6)	89.20	89.49	90.13
S(2)-W-S(4)	79.10	84.29	82.62	N(1)-Ru- $N(5)$	94.67	93.53	93.59
S(2)-W-S(5)	95.89	87.67	80.77	N(1)-Ru- $N(3)$	96.74	96.02	94.69
S(4)-W-S(5)	83.86	74.26	76.32	N(2)-Ru- $N(3)$	89.61	90.49	89.71
S(2)-W-S(3)	105.89	87.67	129.8	N(2)-Ru- $N(4)$	97.11	95.33	95.48
S(3)-W-S(6)	78.22	77.40	78.60	N(3)-Ru- $N(5)$	97.77	97.39	97.93
S(4)-W-S(6)	103.83	113.4	118.1	N(4)-Ru-N(5)	88.02	92.19	91.07
S(3)-W-S(5)	158.21	154.0	149.0	N(2)-Ru-N(6)	97.11	94.77	94.71
S(1)-W-S(4)	156.81	155.0	154.9	N(1)-Ru-N(4)	174.11	172.13	171.93
S(2)-W-S(6)	174.56	161.6	147.1	N(2)-Ru- $N(5)$	171.77	170.09	170.93
C(1)-S(4)-W	111.41	115.5	113.7	N(3)-Ru- $N(6)$	172.51	172.98	173.92
C(2)-S(3)-W	112.77	115.7	112.8				
Torsian angle (°) Torsian angle (°)							
Ru-N(1)-C(1)-S(4)	138.93	173.9	157.8	W-S(3)-C(1)-N(2)	173.89	178.32	152.48
Ru-N(2)-C(2)-S(3)	146.95	142.7	97.3	W-S(4)-C(2)-N(1)	126.83	171.24	156.20

The bond angle of S–W–S in the chelating ligands from the BLYP calculation is 79.25° and 79.92° , and the bond angle of S–W–S on the NCS bridging ligands is 78.22° to 174.56° , while the bond angle of S–W–S between the 5-membered ring WS₂C₂ is 92.44° . Overall, the distorted octahedron of the tungsten metal is between 5.4° and 11.78° . The double bridging ligands –SCN– that connect the tungsten and ruthenium metals form an 8-membered W–(SCN)₂–Ru ring, with a W–S bond length of 2.388 Å and 2.432 Å. Umakoshi et al. have reported the molecule structure of the tungsten bimetallic complex, which is connected to a sulfur atom with a W–S bond length of 2.329 Å to 2.322 Å [16]. Meanwhile, the C–S bond length in the bridging ligand is 1.703 and 1.752 Å, which is shorter than the C–S bond length in the WS₂C₂ rings. However, both of the C–S bonds have lengths in normal range [17]. The two bipyridyl ligands and the two thiocyanate ligands that connect to the ruthenium metal center result in a distorted octahedral geometry with a distorted angle of $5.89 - 8.23^{\circ}$. Both of the bipyridyl ligands are perpendicular to the main plane of the eight-membered rings of W-(SCN)₂-Ru. The Ru–N bond length calculation result is between 2.123-2.138 Å, which is 3.8% longer than the experimental result reported [17]. Meanwhile, the N–Ru–N angle calculation result is between 77.30° and 81.19° .

The molecular structure from the PBE functional calculation results obtained was similar to the BLYP structure; however, the bond lengths and angles are more uniform and closer to the experimental results that have been reported. The W-S bond length is 2.399 - 2.414 Å, and the bond length of the W-S of bridging ligands is 2.602 and 2.617 Å. The S-W-S bond angles of PBE are similar to those obtained with the BLYP calculation results. The Ru-N bond lengths of PBE are shorter than the BLYP calculation result, with the average bond length of 2.09 Å, which is approximately 2% longer than the experimental results [18].

Moreover, the calculations with the BP functional method resulted in a structure with longer bond lengths than the PBE calculation results but slightly shorter than those in the BLYP. The distorted octahedral geometry of the BP calculation result is smallest compared with the BLYP and PBE calculation results. Overall, the PBE method result is considered closest to the experimental value compared with BLYP and BP. For further study, the characterization calculation is only performed with the PBE functional method.

Orbital molecular configuration

Most of the orbital configurations of the monometallic complex molecules have been well described, such as the complex of cis-bis(4,4'-dicarboxylate-2,2'-bipyridine)diisothiocyianate-ruthenium (II) (N3), whose HOMO comes from the Ru metal and isothiocyanate ligand, while its LUMO is mostly derived from bipyridine aromatic rings [19]. In contrast to monometallic complexes, the electronic distribution and molecular orbital configuration of bimetallic complexes have seldom been reported because there are many molecular orbitals involved in the bimetallic complex, causing the orbitals to become irregular and creating difficulty in defining the position of the HOMO and LUMO. Recently, the use of the DFT method, which can describe the molecular orbital configuration of a molecule composed of more than 500 atoms, has led to the successful description of the molecular orbital configuration of large complexes, which contributes to the knowledge of these compounds.

The molecular orbital configuration of the BM bimetallic complex with the PBE calculation results is displayed in Figure 4. There are 339 molecular orbitals involved in the BM bimetallic complex in which the HOMO and LUMO are located at the orbital numbers of 312 and 313, respectively. The HOMO of the BM bimetallic complex is located along the $W(S_2C_2)$ ring with a portion at the ruthenium metal and the -NCS- bridging ligands. The LUMO is located in the bipyridyl and ruthenium metal. The BM complex has overlap energies, as shown in Fig. 4, in which HOMO and HOMO-1, HOMO-2 and HOMO-3, HOMO-4 and HOMO-5, as well as LUMO and LUMO+1, among others, lie at the same energies. This phenomenon always occurs at the C1 molecular symmetry due to the repetitive unit and dimeric nature of the complex [20]. The molecular orbital of LUMO+1 up to LUMO+4 also fully lies in the bipyridine ligands and the ruthenium metal center, while all of LUMO+5 and LUMO+6 lies at the tungsten metal and the SCN bridging ligands. Meanwhile, HOMO-1 to HOMO+4 are primarily spread over the tungsten metal, along with the dithiolene ligand with some at ruthenium and the NCS bridging ligands, while HOMO-5 and HOMO-6 lie along the two metal centers and the bridging ligands.

The LUMO to LUMO+2 band gap energy is smaller than that of HOMO to HOMO-2, indicating that it is easier to reduce than to oxidize the BM complex. Furthermore, oxidation occurs more easily on tungsten metal because the HOMO and HOMO-1 are mostly lying at the tungsten and the dithiolene ligands. Reduction occurs more easily at bipyridine and the ruthenium metal. This result is compatible with the cyclic voltammetry analysis results that have been previously reported [7]. The HOMO-LUMO band gap energy calculation using PBE (0.383 eV) was found as the smallest compared with the band gap energy from the BLYP (0.402 eV) and BP (1.339 eV) methods.

Optical properties

The optical properties of the bimetallic complex were studied from the TD-DFT calculation using the PBE functional of the GGA method. Using this technique, the optical properties, which are difficult to identify experimentally, could be easily solved. Table 3 summarizes the 12 lowest singlet and triplet excitations under vacuum. The lowest excitation energy of the singlet state is the excitation of an electron from the HOMO to the LUMO, which lies at the $312 \rightarrow 313$ molecular orbital. This excitation appears as an absorption peak at 2964 nm with an energy of 0.42 eV, which is absorption of 1 MMCT. This absorption is wider than that of the two constituent complexes. The highest oscillator strength is the excitation of the $310 \rightarrow 314$ orbitals (HOMO-3 \rightarrow LUMO), which is the excitation of 1 MLCT at an absorption wavelength of 847 nm with a 1.46 eV excitation energy. While at the triplet state (3 MMCT), the electron excitation of HOMO \rightarrow LUMO occurs at a lower energy wavelength, with an energy of 0.39 eV. Table 3 shows that the twelfth position of excitation of the lowest singlet and triplet in the bimetallic complex molecular excitation is derived from metal to metal and metal to ligand. The calculations results show that the BM absorbs light energy up to the near IR region. These results also agree with the experimental results in which the absorption of light of the bimetallic complex BM was higher than the monometallic complexes (M1 & M2) and N3 commercial sensitizer [7].

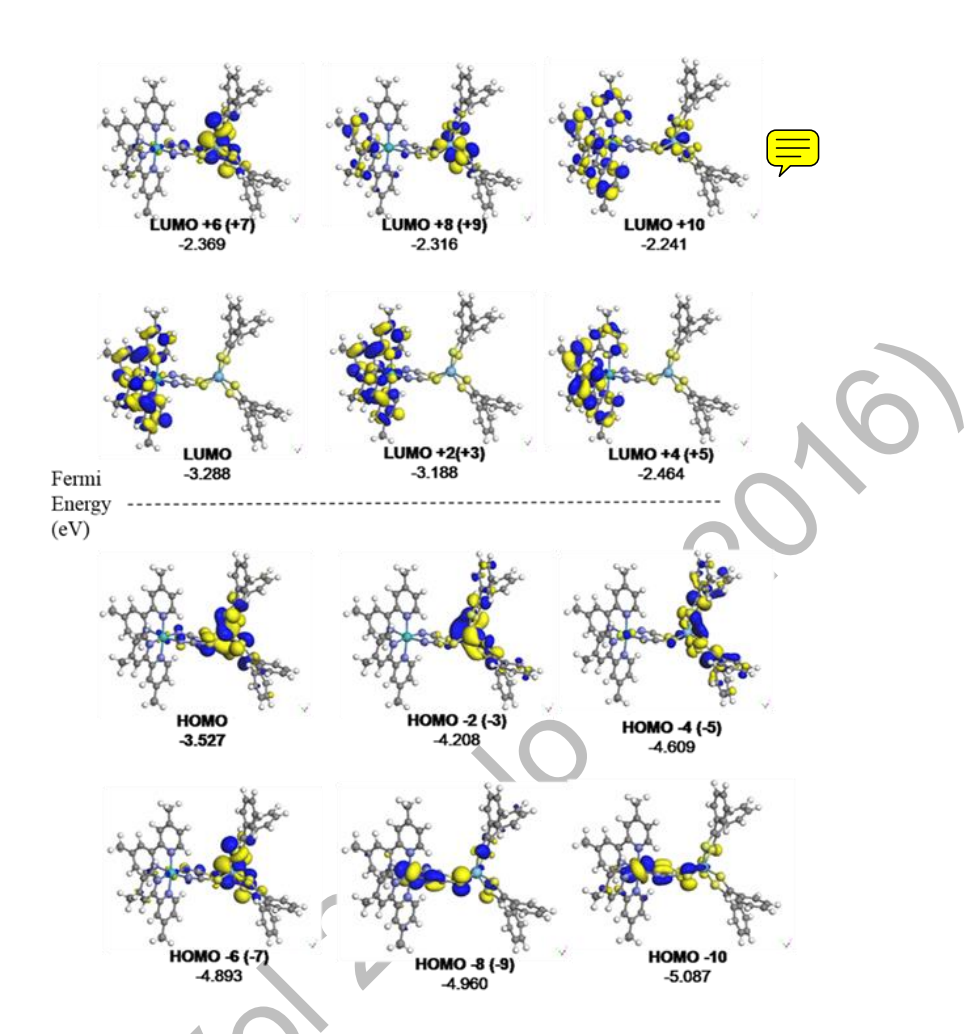


Figure 4. Molecular orbital configuration of BM

Table 3. Summary of 12 lowest singlet TDDFT excitations energies for optical transitions of BM in vacuum

Singlet	Overlap	Excitation			Oscilator	
From To	%	eV	Nm	На	strength	
$312 \rightarrow 313$	0.19	0.42	2964	0.015370	0.009184	
$312 \rightarrow 314$	0.19	0.50	2475	0.018411	0.004193	
$311 \rightarrow 313$	0.10	0.97	1272	0.035811	0.000440	
$311 \rightarrow 314$	0.12	1.07	1163	0.039175	0.005050	
$312 \rightarrow 315$	0.11	1.22	1017	0.044806	0.000296	
$312 \rightarrow 316$	0.64	1.34	928	0.049115	0.000337	
$310 \rightarrow 313$	0.13	1.40	883	0.051610	0.006453	
$312 \rightarrow 317$	0.61	1.43	868	0.052498	0.006724	
$310 \rightarrow 314$	0.15	1.46	847	0.053778	0.014428	
$312 \rightarrow 318$	0.47	1.54	806	0.056517	0.006252	
$312 \rightarrow 319$	0.26	1.58	785	0.058034	0.000703	
$312 \rightarrow 320$	0.14	1.61	771	0.059124	0.013394	

Table 3 (cont'd).	Summary of 12 lowest singlet TDDFT excitations energies for optical transitions
	of BM in vacuum

Triplet	Overlap	Excitation			Oscilator	
From To	%	eV	Nm	Ha	strength	
$312 \rightarrow 313$	0.19	0.39	3176	0.014347	0.0	
$312 \rightarrow 314$	0.19	0.48	2585	0.017628	0.0	
$311 \rightarrow 313$	0.10	0.97	1278	0.035643	0.0	
$311 \rightarrow 314$	0.12	1.06	1171	0.038918	0.0	
$312 \rightarrow 315$	0.11	1.21	1021	0.044616	0.0	
$312 \rightarrow 316$	0.64	1.22	1018	0.044771	0.0	
$310 \rightarrow 313$	0.13	1.29	961	0.047400	0.0	
$312 \rightarrow 317$	0.61	1.33	932	0.048888	0.0	
$310 \rightarrow 314$	0.15	1.42	874	0.052117	0.0	
$312 \rightarrow 318$	0.47	1.43	866	0.052628	0.0	
$312 \rightarrow 319$	0.26	1.55	802	0.056782	0.0	
$312 \rightarrow 320$	0.14	1.57	788	0.057822	0.0	

Conclusion

The geometrical structure of the BM bimetallic complex was successfully modeled using the DFT calculation technique with the DMol³ Material Studio software package. This technique can be used to build the molecular structure, although it was unsuccessful at growing a quality crystal for X-ray single crystal analysis. The bond lengths and angles of the calculation results using the PBE functional of the GGA method had the most similar appearance to the experimental data. From the calculation result, 339 molecular orbitals were involved in the complex in which the HOMO and LUMO orbitals were located at orbital numbers 312 and 313, respectively. The band gap energy between the HOMO and LUMO was 0.383 eV. The HOMO of the complex was mostly derived from the W(S_2C_2) rings with a portion from the Ru metal and the NCS bridging ligands. The LUMO was primarily derived from the bipyridyl ligands and the Ru metal. The optical properties of the complex analysis from the TD-DFT calculation shows that the electronic absorption of the complex can reach up to 2964 nm and is wider compared with the absorption area of the monometallic complex starting materials, which is 902 nm for *cis*-W($S_2C_2Ph_2$)₂(CO)₂ (M2) and 1652 nm for *cis*-[Ru(dmbpy)₂NCS₂] (M1).

Acknowledgement

The authors would like to acknowledge the Universiti Kebangsaan Malaysia for sponsoring this project under the UKM-GUP-07-30-190 and FRGS/1/2015/SG01/UKM/03/1 research grants.

References

- 1. Guo, P., Ma, R., Guo, L., Yang, L., Liu, J., Zhang, X., Pan, X. and Dai, S. (2010). Theoretical study on the electronic absorption spectra and molecular orbitals of ten novel ruthenium sensitizers derived from N3 and K8. *Journal of Molecular Graphics and Modelling*, 29: 498 505.
- 2. Islam, M. S. and Fisher, C. A. J. (2014). Lithium and sodium battery cathode materials: computational insights into voltage, diffusion and nanostructural properties. *Chemical Society Reviews*, 43: 185 204.
- 3. Mehmood, F. and Pachter, R. (2014). Density functional theory study of chemical sensing on surfaces of single-layer MoS2 and graphene. *Journal of Applied Physics*, 115: 164302.
- 4. Khan, W., Reshak, A. H., Ahmad, K. R. and Alahmed, Z. A. (2014) Magnetic and thermoelectric properties of three different atomic ratio of Bi/Mn in BiMn₂O₅: DFT approach. *Journal of Magnetism and Magnetic Materials*, 369: 234 242.
- Shariatinia, Z. and Shahidi, S. (2014). A DFT study on the physical adsorption of cyclophosphamide derivatives on the surface of fullerene C₆₀ nanocage. *Journal of Molecular Graphics and Modelling*, 52: 71 – 81.

- 6. Young, D. C. (2001). Computational chemistry: A practical guide for applying techniques to real-world problems, John Wiley & Sons, Inc., New York.
- 7. Arifin, K., Daud, W. R. W. and Kassim, M.B. (2013). Optical and photoelectrochemical properties of a TiO₂ thin film doped with a ruthenium-tungsten bimetallic complex. *Ceramics International* 39: 2699 –2707.
- 8. Arifin, K., Daud, W. R. W. and Kassim, M. B. (2014) A novel ruthenium-tungsten bimetallic complex dyesensitizer for photoelectrochemical cells application. *Sains Malaysiana*, 43 (1): 95 101.
- 9. Becke, A. D. (1988). Density-functional exchange-energy approximation with correct asymptotic behavior. *Physical Review*, 38: 3098 3100.
- 10. Parr, R. G. and Yang, W. (1989). Density-functional theory of atoms and molecules, Oxford Univ. Press, Oxford.
- 11. Perdew, J. P., Burke, K., and Ernzerhof, M. (1996). Generalized gradient approximation made simple. *Physical Review Letters*, 77: 3865.
- 12. Sokolov, A. N., Atahan-Evrenk, S., Mondal, R., Akkerman, H. B., Sánchez-Carrera, R. S., Granados-Focil, S. J., Schrier, S. C., Mannsfeld, B., Zoombelt, A. P., Bao, Z. and Aspuru-Guzik, A. (2011). From computational discovery to experimental characterization of a high hole mobility organic crystal. *Nature Communications*, 2: 437 445.
- 13. Wilson, G. J. and Will, G. D. (2010). Density-functional analysis of the electronic structure of tris-bipyridyl Ru(II) sensitisers. *Inorganic Chimica Acta* 363(8): 1627 1638.
- 14. Delley, B. (2010). Time dependent density functional theory with DMol³. *Journal of Physics: Condensed Matter*, 22: 384208.
- 15. Eran, B. B., Singer, D., Pickardt, J. and Praefcke, K. (2001). Thiocyanato-bridged platinum heterocycles: structure and properties of disc-like metallomesogens. *Journal of Organometallic Chemistry*, 620: 249 -255.
- 16. Umakoshi, K., Nishimoto, E., Sokolov, M., Kawano, H., Sasaki, Y. and Onishi, M. (2000). Synthesis, structure, and properties of sulfido-bridged dinuclear tungsten(V) complex of dithiolene, $(Pr_4N)_2[W_2(m-S)_2\{S_2C_2(CO_2Et)_2\}_4]$. *Journal of Organometallic Chemistry*, 611: 370 375.
- 17. Allen, F. H., Kennard, O., Watson, D. G., Brammer, L., Orpen, A. G. and Taylor, R. J. (1987). Tables of bond lengths determined by X-Ray and neutron diffraction. Part 1. Bond lengths in organic compounds, *Journal of the Chemical Society, Perkin Transactions 1*, 112: 1 19.
- 18. Arifin, K., Daud, W. R. W. and Kassim, M. B. (2014). A DFT analyses for molecular structure, electronic state and spectroscopic property of a dithiolene tungsten carbonyl complex. *Spectrochimica Acta Part A: Molecular and Biomolecular Spectroscopy*. 124: 375 382.
- 19. Nazeeruddin, M. K., Angelis, F. D., Fantacci, S., Selloni, A., Viscardi, G., Liska, P., Ito, S., Takeru, B. and Grätzel, M. (2005). Combined experimental and DFT-TDDFT computational study of photoelectrochemical cell ruthenium sensitizers. *Journal of the American Chemical Society*, 127: 16835 16847.
- 20. Rabias, I., Howlin, B. J., Provata, A. And Theodorou, D. (2000). Modelling of structural and vibrational properties of poly(p-phenylene) and polypyrrole using molecular orbital methods. *Molecular Simulation* 24: 95 105.